Indian Journal of Biochemistry & Biophysics
Vol. 63, January 2026, pp. 19-28
DOI: 10.56042/ijbb.v63i1.16424

Interaction of 7,8-dihydroxycoumarin with a biopolymer bromelain: Synthesis, spectroscopic and molecular docking insights

Sourav Pakrashy[1,3], Prakash K Mandal[2], Sourav Misra[1], Pawan K Maurya[4], Malay Dolai[3]* & Anjoy Majhi[1]*

[1]Department of Chemistry, Presidency University, 86/1 College Street, Kolkata-700 073, West Bengal, India

[2]Department of Chemistry, University of Calcutta, Kolkata-700 003, West Bengal, India

[3]Department of Chemistry, Prabhat Kumar College, Purba Medinipur-721 404, West Bengal, India

[4]Indian Council of Medical Research-Centre for Ageing and Mental Health, Division of Non-Communicable Diseases, Kolkata-700 091, West Bengal, India

Received 15 January 2025; *revised 04 July 2025*

Dihydroxycoumarins which are present in nature as natural products in medicinal plants used for herbal treatment, have numerous pharmacological and therapeutic potentials. They can be developed as promising components of treatment in various medicinal fields. Regardless of several advantages, they have a few disadvantages like low molecular weight and low solubility which lowers the appropriate bioavailability. The strategy is to identify effective intake with a carrier for oral drug delivery. In this paper, we synthesized daphnetin (7,8-dihydroxycoumarin) which has various medicinal properties in a pot-economical multicomponent domino fashion, and explored its biophysical interaction with cysteine protease enzyme bromelain for the very first time using steady-state fluorescence and temperature variation experimentally at pH 7.4 since it has a proven record of enhancing the efficacy of drugs. The binding constant (or stability constant) of the bromelain-daphnetin interaction is determined from the double-logarithmic plot at three different temperatures, 288K, 298K, and 308K. The change of enthalpy and entropy revealed the major forces of interaction. Thus, bromelain can be used as a drug carrier for daphnetin.

Keywords: Bromelain, Dihydroxycoumarins, Docking, Fluorescence, Synthesis

Natural products have been documented as mediators for handling human ailments throughout the sphere for centuries. Foundations of natural products are diverse which embraces vertebrates, invertebrates, plants, microorganisms, and marine organisms[1]. Variety in natural chemical bases aids as an imperative cenote of prospective bio-active phytoconstituents in the progress of novel leads by providing unique synthons for fresh drugs, in addition to paths for structural building to harvest highly potent, harmless, and cheap drugs. 25% of total drugs are contributions from medicinal plant-derived natural products[2] while over 60% of all clinically approved drugs are encouraged from natural products. To name a few, the essential strategy of metformin cast-off in the supervision of diabetes is encouraged by Galegine, a phytocompound of *Galega officinalis* L.[3] phytocompound Papaverine isolated from Papaver somniferum, surfaced approach for the progress of the semisynthetic drug verapamil which helps in hypertension[4].

Dihydroxy-coumarins which are found in medicinal plants (Fig. 1), for the continuation of our project[5]. They have two binding sites and are also active. These dihydroxy-coumarins are medicinally active. Daphnetin (DAPH), a dihydroxycoumarin derivative mostly extracted from Daphne species, is a biologically active phytocompound with ample bioactivities including antioxidant activity, anti-inflammatory response, neuroprotective effect, anti-malarial activity, analgesic activity, antipyretic action, anti-bacterial activity, anti-arthritic response, nephroprotective, hepatoprotective, anti-tumor, and anticancer activities. A wide range of studies have been conducted exploring the significance and therapeutic potential of DAPH. In this paper, it is synthesized in a pot economical manner.

Combinations of drug moieties with bromalein (BMLN) a cysteine protease enzyme seem to seek attention in the ground of drug designand delivery.

*Correspondence:
E-mail: anjoy.chem@presiuniv.ac.in (AM);
dolaimalay@yahoo.in (MD)
Suppl. data available on respective page of NOPR

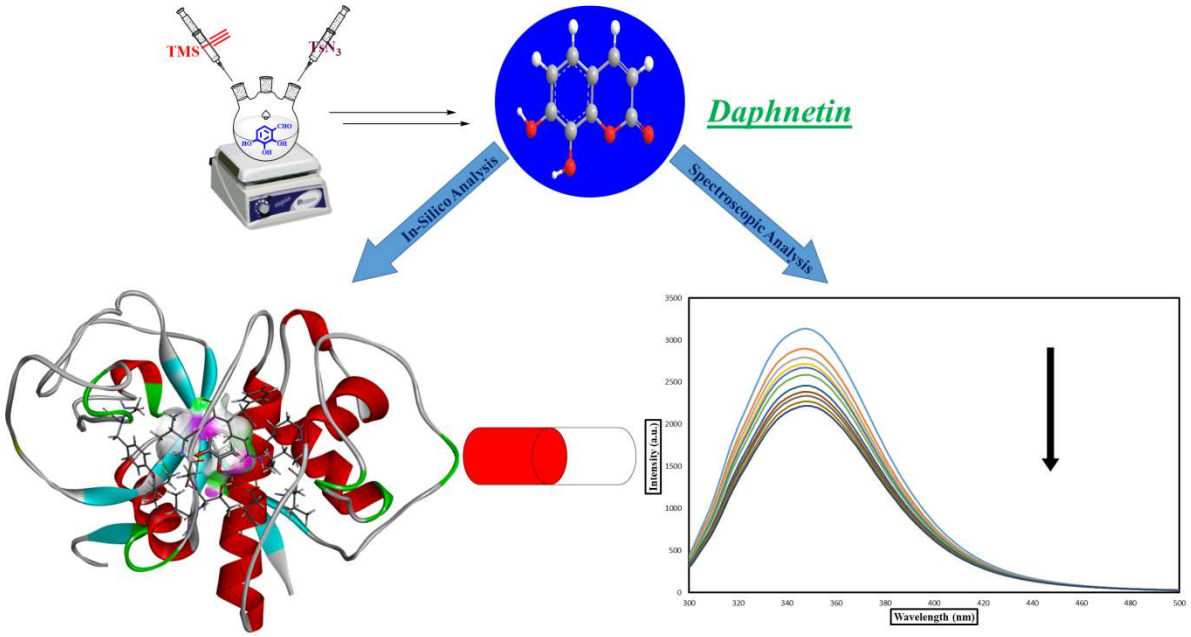

Graphical abstract

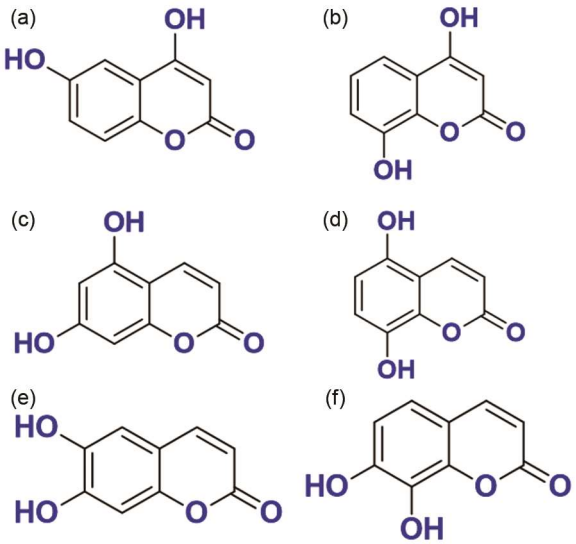

Fig. 1 — The dihydroxycoumarins present in medicinal plants (a) 4,6 –dihydroxycoumarins; (b) 4,8-dihydroxycoumarins; (c) 5,7-dihydroxycoumarin; (d) 5,8-dihydroxycoumarin; (e) 6,7-dihydroxycoumarin; and (f) 7,8-dihydroxycoumarin

Ali *et al*. (2014) determined that the combination of 0.9 mg/ml of crude BMLN and 2.5 mg/ml of Ampicloxacillin, enhanced the efficacy of the antibiotic[6]. Ghensi *et al*. also determined that dexamethasone sodium phosphate (20 ng/mL) when combined with BMLN (20 ng/mL) resulted in increased biosynthesis of hyaluronan and collagen along with increased release of anti-inflammatory cytokines[7]. The combination of BMLN and acetylcysteine aids the dissociation of tumors[8] also a combination of BMLN and acetylcysteine can show synergistic action against glycoproteins of SARS-CoV-2 by breakage of its glycosidic linkages and S-S bonds[9]. Hence, an interaction study with our dihydroxy-coumarin with BMLN can be an important investigation for drug design and development.

Experimental Section

Materials

The reagents used here, were hailed from sigma-aldrich spectrochem chemicals, respectively as reagent AR grade. In addition, reactions were performed in an oven-dried glass vial or cuvette, fitted with a knockback silicon-made cap which is suitable for cavitation during sonication without stirring the magnetic bar. Petroleum ether used in our experiments was in the boiling range of 60-80°C. Column chromatography was performed on silica gel (100-200 mesh). TLC was done on aluminium sheets pre-coated with silica gel (with binder, 300 meshes, Merck). The 1H-NMR spectrum was taken in DMSO-d_6 with TMS as an internal standard on the Bruker Supercon NMR spectrometer (Model: AV 300 Digital) and Bruker Supercon NMR spectrometer (Model: AV 400 Digital). The chemical shifts were reported as δ values (ppm) relative to tetramethylsilane.

Synthesis of 7,8-dihydroxy coumarin (Daphnetin)

In this work, we have used the reagent with a suitable catalyst (scheme 1). Tosyl azide was prepared

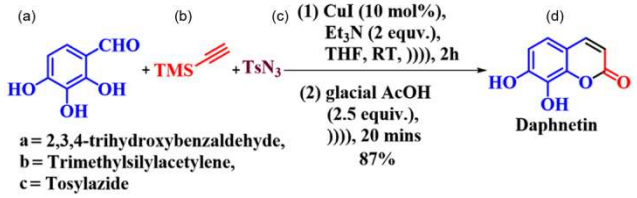

Scheme 1 — Modified synthetic technique of 7,8-dihydroxycoumarin/ Daphnetin (DAPH)

by standard protocol (18) from tosyl chloride and sodium azide.

We have approached a slightly modified synthetic protocol of DAPH (d), inspired by the work of S.-L. Cui *et al.*[19], but in a more sustainable way. At the beginning, 2,3,4-trihydroxy benzaldehyde (a) [0.5 mmol, 77 mg], trimethylsilylacetylene (b) [0.6 mmol, 0.085 mL], and tosylazide (c) [0.6 mmol, 0.13 mL], were taken in a clean and dry 10 mL reaction vessel along with CuI [0.05 mmol, 9.5 mg] and triethylamine [1 mmol, 0.14 mL] and finally, DCM (2.5 mL) was added as the solvent[20,21]. The reaction mixture was kept stirring under the cavitation of a sonication bath and monitored by TLC checking. After 2 h elapse, the first step of the reaction was completed by producing iminocoumarin as an intermediate. Then, glacial acetic acid (2.5 equiv.) was charged into the same reaction vessel for 20 min under sonication for conducting hydrolysis to obtain our target product DAPH (d) with 87% yield after isolation by column chromatography. From extensive mechanistic studies by different groups[22,23], it has been established that iminocoumarins were rendered by Cu(I) catalyzed Azide-Alkyne-Cycloaddition (CuAAC) *via* ketenimine intermediate from salicylaldehydes, alkynes, and tosylazides as starting materials[24,25].

^{1}H-NMR (400MHz, CD_3OD): 6.16 (1H, J = 9.6, d), 6.79 (1H, J = 8.4, d), 6.97 (1H, J = 8.4, d), and 7.81 (1H, J = 9.6, d) ppm (Suppl. Fig. S1).

^{13}C-NMR (100MHz, CD_3OD): 110.80, 112.23, 112.52, 118.78, 132.11, 143.58, 145.31, 149.73, and 162.05 ppm (Suppl. Fig. S2).

Molecular docking

The computational docking of the natural product which is protein-ligand binding energy (ΔG) analysis was performed using AutoDock Vina[26] as an extension in UCSF Chimera[27].

The structure of BMLN enzyme was taken from the Protein databank (RCSB PDB) (http://www.rcsb.org/pdb). For BMLN, 1W0Q (PDB-ID) in PDB format[28]. The macromolecule and binder preparation was completed agreeing to our previous published works[16,28-33]. The charges were assigned as per the ANTECHAMBER algorithm [34], the energy-minimization was completed through swiss pdb (SPDBV)[35] viewer, and ligands were adjusted with the Gasteiger algorithm[36].

ADMET prediction

In silico ADME analysis was conducted using pkCSM[37] to investigate physico-chemical properties of the potent hits, such as water solubility, lipophilicity, druglikeness, and pharmacokinetics.

Fluorescence Spectroscopy

The steady-state Fluorescence emission spectrum in every case was recorded using an F-4700 Hitachi spectrofluorimeter, prepared with a 1 cm path-length quartz cuvette-cell and circulating water bath. All the experiments were performed in the micromolar concentration range to avoid the aggregation and inner filter effect. The solution of bromelain (BMLN) (5.1 µM) was titrated with DAPH (0-2 µM). The excitation wavelength was set at 290 nm. The excitation and emission bandpass were maintained at 10 nm and 5 nm, respectively. F_0 and F in all the cases were calculated considering the area under the emission curve of the corrected fluorescence spectrum.

Results and Discussion

Result of synthesis

The scheme above 1 was executed as a model reaction for optimization. [a]The reaction condition: 1,2,4-trihydroxy benzaldehyde (a) [0.25 mmol], Trimethylsilylacetylene (b) [0.3 mmol], and Tosyl azide (c) [0.3 mmol] were taken along with suitable Cu(I) or Cu(II) catalyst (in mol%) and triethylamine (0.5 mmol) in a solvent at RT for a certain completion time (generally 240 min *i.e.*, 4 h) under sonication to obtain the desired product Daphnetin (d). [b]Equivalency of the base w.r.t. starting material a. [c]Yield% calculated after isolation and purification by column chromatography. [d]No Reaction. [e]Not Detected the desired product. [f]Gram scale production.

An extensive investigation was performed to obtain the most productive conditions to achieve DAPH (d) under the belt of this protocol. Applying the optimized condition (entry 15, Table 1), we synthesized DAPH in a pot-economic sustainable fashion with approximately 87% yield after purification by column chromatography and identified

Table 1 — Optimization table for synthesizing DAPH[a]

Sl.	Catalyst	Mol%	Solvent	Base with Equiv[b]	Sonicator Temp. (°C)	Sonication Time (min)	Yield%[c]
1.	-	-	THF	Et_3N (2)	RT	240	NR[d]
2.	CuI	10	THF	Et_3N (2)	RT	240	86
3.	CuI	10	Toluene	Et_3N (2)	RT	240	71
4.	CuI	10	MeCN	Et_3N (2)	RT	240	65
5.	CuI	10	DCM	Et_3N (2)	RT	240	81
6.	CuI	10	DMSO	Et_3N (2)	RT	240	52
7.	CuI	10	EtOH	Et_3N (2)	RT	240	ND[e]
8	CuCN	10	THF	Et_3N (2)	RT	240	80
9	$Cu(OAc)_2$	10	THF	Et_3N (2)	RT	240	69
10	$CuBr_2$	10	THF	Et_3N (2)	RT	240	77
11	CuI	05	THF	Et_3N (2)	RT	240	84
12	CuI	15	THF	Et_3N (2)	RT	240	87
13	CuI	10	THF	Et_3N (1)	RT	240	78
14	CuI	10	THF	Et_3N (3)	RT	240	86
15	CuI	10	THF	Et_3N (2)	RT	120	87
16	CuI	10	THF	Et_3N (2)	50°C	120	84
17	CuI	10	THF	Et_3N (2)	10°C	120	82
18[f]	CuI	10	THF	Et_3N (2)	RT	120	85

by ^{1}H-NMR. The detailed investigation report for optimization reaction is provided in the ESI.

Fluorescence quenching

The tryptophan (Trp) emission of free BMLN was quenched (Fig. 2) with the regular adding of DAPH with a redshift. This red shift indicates a reduction in hydrophobicity of the Trp environment[10]. Therefore, it is seen that during the interaction, the Trp moiety of BMLN gradually shifts towards the solvent. Hence, the change in conformation occurring through the binding of DAPH with BMLN leads to exposure of the Trp residue[11].

There are two most commonly used mechanisms for quenching-static and dynamic. In the event of static quenching, fluorophore forms a non-fluorescent complex with a quencher in the ground state, thus reducing the fluorescence intensity of fluorophore-quencher system from that of free fluorophore. In the case of dynamic quenching, the quencher forms a complex with a fluorophore in the excited state and removes a fraction of excited fluorophore molecules, thereby reducing fluorescence intensity[11,12].

To have quantitative knowledge about fluorescence quenching, the Stern-Volmer equation (Eq. 1) is most widely accepted.

$$\frac{F_0}{F} = 1 + K_{SV}[Q] = 1 + k_q \tau_0 [Q] \quad \ldots (1)$$

F_0 and F represent fluorescence intensities of the fluorophore (here BMLN) in the non-attendance and the attendance of the quencher, Q (here DAPH). [Q] is the molar concentration of Q and K_{sv} is known as the Stern-Volmer quenching constant, the Stern-Volmer plots are given in (Fig. 3). The term k_q is called the bimolecular quenching constant and τ_0 is called the average lifetime of fluorophore in the non-attendance of a quencher[12]. The following table (Table 2) comprises the experimental values of K_{sv} and k_q for the binding of BMLN with DAPH at 288K, 298K, and 308K. Here τ_0 of Trp residue of BMLN is taken as 10^{-8} sec[13].

From Table 2 it is detected that in all cases the assessment of k_q is more than 2×10^{10} $M^{-1}s^{-1}$. This specifies the incident of static-quenching[14,15]. Thus, DAPH undergoes complex formation with BMLN in the ground state. This is further supported by witnessing the tendency of decreasing K_{sv} with increasing temperature. As temperature increases, the extent of dissociation of the BMLN-quencher complex decreases, and hence, the extent of quenching increases, so K_{sv} increases[14,16].

Binding constant and number of binding sites

The Eq. 2 is used for the assessment of the binding-constant of the ligands with protein macromolecules.

$$log\frac{(F_0 - F)}{F} = logk_b + nlog[Q] \quad \ldots (2)$$

Here k_b represents the binding constant, and n represents several binding sites. F_0 and F represent

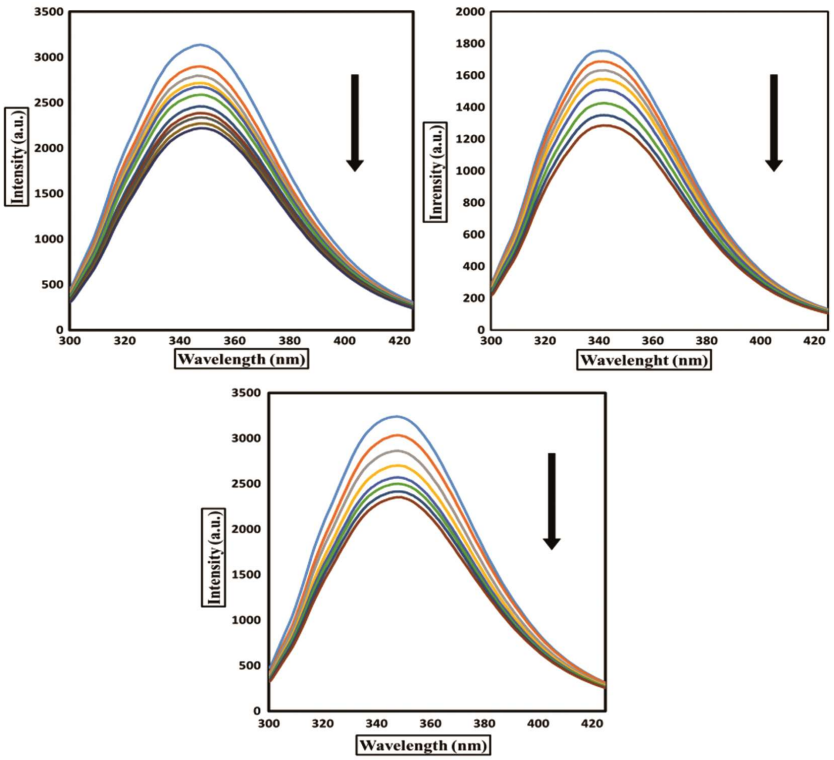

Fig. 2 — Steady-state Fluorescence spectrum of the titration experiments between free BMLN (5μM) and increasing concentration of DAPH in aqueous phosphate buffer (pH 7) at (a) 288K; (b) 298K; and (c) 308K

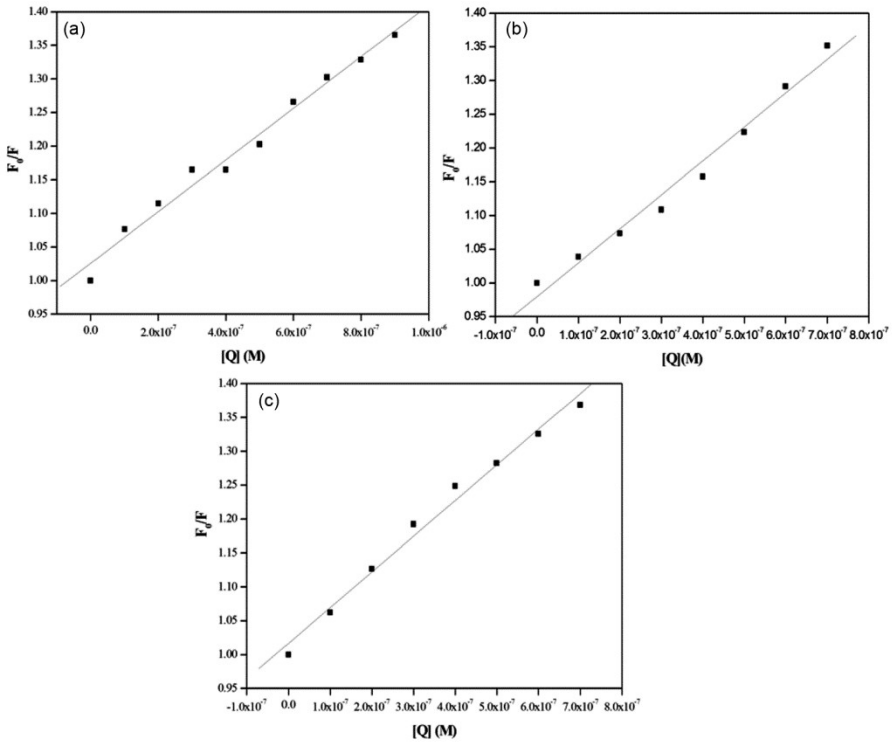

Fig. 3 — Stern-Volmer plots for (a) Free BMLN (5 μM) and increasing concentration of DAPH in aqueous phosphate buffer (pH 7) at 288K; (b) Free BMLN (5μM) and increasing concentration of DAPH in aqueous phosphate buffer (pH 7) at 298K; and (c) Free BMLN (5 μM) and increasing concentration of DAPH in aqueous phosphate buffer (pH 7) at 308K

fluorescence strengths of the fluorophore (here BMLN) in the non-appearance and in the appearance of the quencher, Q (here DAPH)[11,16]. The following table (Table 3) comprises the experimental values of K_b for the binding of BMLN with DAPH at 288K, 298K, and 308K.

Table 2 — Stern-Volmer quenching constants and bimolecular quenching constants for the interactions of BMLN with DAPH at 288K, 298K and 308K

System	Temperature (K)	K_{sv} (M^{-1})	k_q ($M^{-1}s^{-1}$)	R^2
BMLN And DAPH	288	3.84×10^5	3.84×10^{13}	0.98
	298	5.03×10^5	5.03×10^{13}	0.98
	308	5.27×10^5	5.27×10^{13}	0.98

Table 3 — Binding constants and number of binding sites for interaction of BMLN with DAPH at 288K, 298K, 308K

System	Temperature (K)	K_b (M^{-1})	N	R^2
BMLN And DAPH	288	4.21×10^5	1	0.985
	298	3.43×10^5	0.997	0.992
	308	2.07×10^5	0.928	0.993

In the case of DAPH, moderately strong binding affinity is observed (binding constant values lie in the order of 10^5). For DAPH, the binding constant value decreases with the rise in temperature signifying that elevated temperature tips to destabilization of the complex formed between DAPH and BMLN at higher temperatures[14]. The double-logarithmic plots of free BMLN (5 μM) and increasing concentration of DAPH in aqueous phosphate buffer (pH 7) at 288K, 298K, and 308K are given in (Fig. 4).

Thermodynamic parameters

To comprehend the thermodynamics of BMLN-DAPH binding, van't Hoff equation (Eq. 3) is used. Plot of lnk_b *vs* 1/T gives a straight line, (Fig. 5). From the slope and the intercept, the values of ΔH and ΔS are determined.

$$lnk_b = \frac{-\Delta H}{RT} + \frac{-\Delta S}{R} \quad \text{... (3)}$$

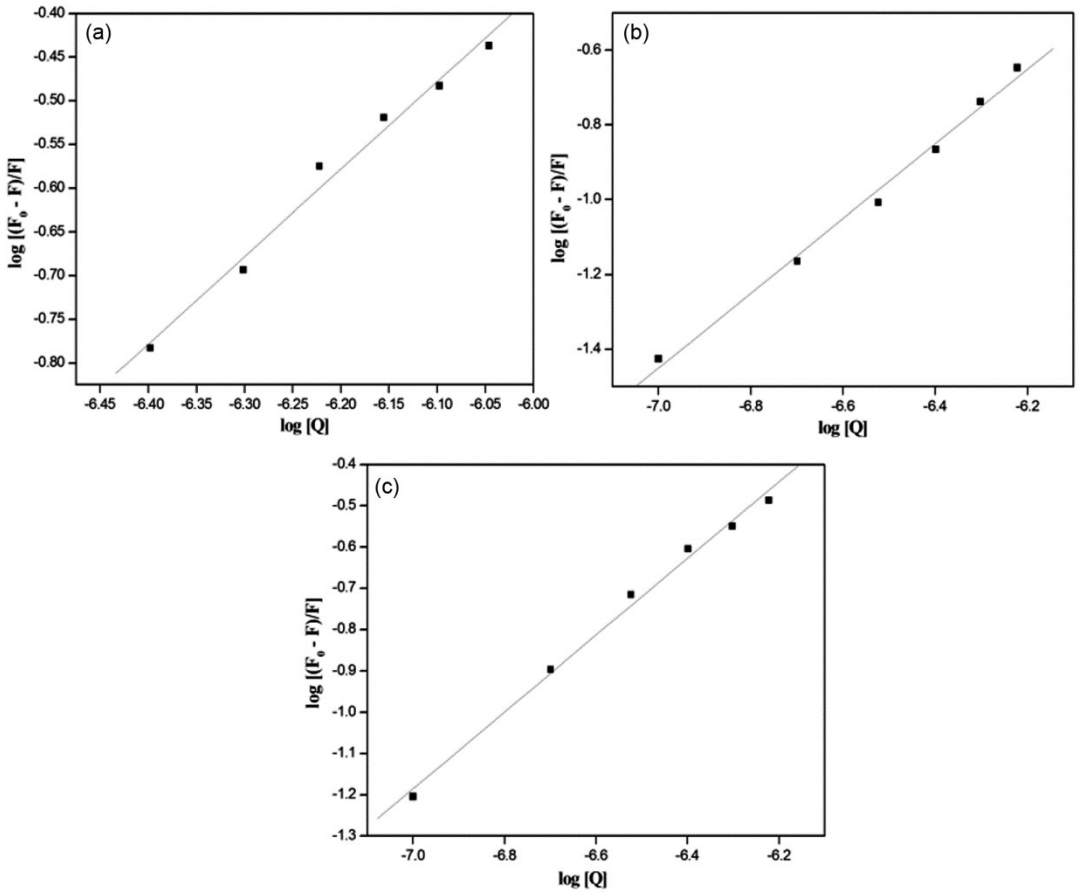

Fig. 4 — Double-logarithmic plots for (a) Free BMLN (5 μM) and increasing concentration of DAPH in aqueous phosphate buffer (pH 7) at 288K; (b) Free BMLN (5 μM) and increasing concentration of DAPH in aqueous phosphate buffer (pH 7) at 298K; and (c) Free BMLN (5 μM) and increasing concentration of DAPH in aqueous phosphate buffer (pH 7) at 308K

Where K_b is the binding constant, ΔH represents a change in enthalpy and ΔS represents a change in entropy during the interaction between BMLN and the DAPH[13]. As per the suggestion of Subramanian and Ross, the signs of ΔH and ΔS indicates the nature of binding forces. If both ΔH and ΔS are negative, then van der Waals interaction and H-bonding are considered primary binding forces in the protein-ligand complex. If both ΔH and ΔS are positive, then hydrophobic forces are considered primary binding forces in the protein-ligand complex. Finally, if only ΔH is negative and ΔS is positive, then electrostatic interactions are considered as primary binding forces in the protein-ligand complex[17], but a very small positive ΔS value with a high ΔH value refers to strong H-bonding.

The spontaneity of the interaction is predicted by a change in Gibbs free energy (ΔG), which is related to ΔH and ΔS as per the following equation (Eq. 4).

$$\Delta G = \Delta H - T\Delta S \quad \ldots (4)$$

From Table 4 it is observed that, in all cases the ΔG is negative, indicating that the interactions are spontaneous (5). The signs of ΔH and ΔS indicate that DAPH binds with BMLN using van Der Waals interaction and hydrogen bonding forces of attraction in equal magnitude.

Docking studies

The link between the mark protein (PDB-ID: 1W0Q) and DAPH is assessed by employing molecular docking. The designs reveal the highest free energy change for these interactions as ΔG = - 7.1 Kcal/mol (Table 5) of DAPH for protein 1W0Q inside a grid box of -2.61 × 4.22 × -0.76 Å with dimensions 52 × 36 × 35 Å along three axes (Fig. 6). From the 2D diagram Figure 6 it is evident that three strong hydrogen bonds of bond length 2.98, 2.24, and 2.08 Å formed between DAPH and 33rd alanine residue (one hydrogen bond) and 36th glutamic acid residue (two hydrogen bonds) of protein 1W0Q (Fig. 6).

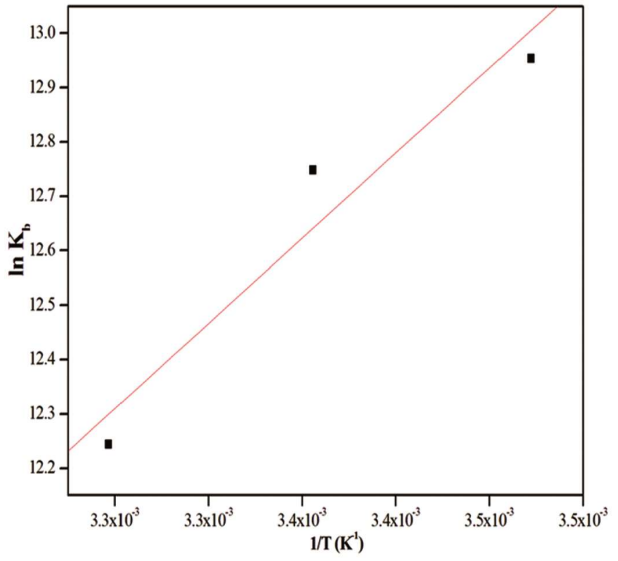

Fig. 5 — van't Hoff plot for BMLN and DAPH system, in aqueous phosphate buffer (pH 7)

Docking Results

ADMET Prediction Results

The result from pkCSM is agreeable as DAPH does not violate any of Lipinski's rule of drug-likeness properties and it has high gastrointestinal absorption, no blood-brain-barrier (BBB) permeant property, DAPH does not inhibit any of the cytochrome P50 enzymes but CYP1A2, it is not a P-gp substrate, it has no AMES toxicity, and also not an h-ERG inhibitor, which makes it orally admissible to people.

Table 4 — Thermodynamic parameters and nature of interacting forces for the interaction of BMLN with DAPH at 288K, 298K, 308K

System	Temperature (K)	ΔH (kJ mol^{-1})	ΔS (J K^{-1} mol^{-1})	ΔG (kJ mol^{-1})	Nature of interacting forces
BMLN And DAPH	288	-26.06	17.73	-31.02	van Der Waals interaction and hydrogen bonding
	298			-31.59	
	308			-31.53	

Table 5 — Results of the Docking of DAPH and target protein 1W0Q

Name of Dihydroxycoumarins	PDB ID	Docking Score (Kcal/mol)
1) DAPH	1W0Q	-7.1

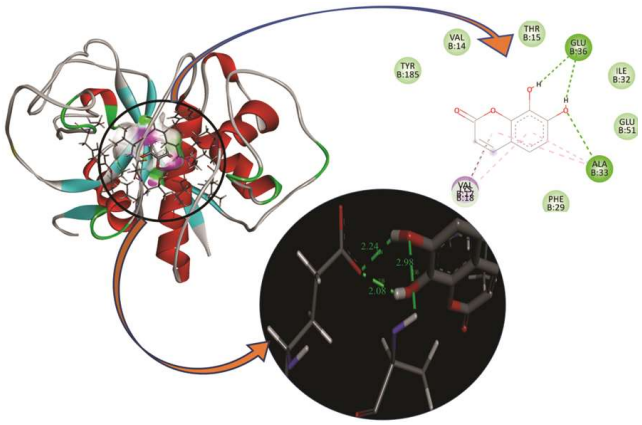

Fig 6 — Different Docking Poses of 7,8-dihydroxycoumarin (DAPH) with 1W0Q

Table 6 — ADMET Prediction Results of DAPH

Property	Model Name	Predicted Value
Absorption	Water-solubility	-2.583
Absorption	Caco2-permeability	0.659
Absorption	Intestinal-absorption-(human)	92.489
Absorption	Skin—Permeability	-2.754
Absorption	P-glycoprotein—substrate	No
Absorption	P-glycoprotein-I-inhibitor	No
Absorption	P-glycoprotein-II-inhibitor	No
Distribution	VDss-(human)	0.324
Distribution	Fraction-unbound-(human)	0.51
Distribution	BBB-permeability	0.062
Distribution	CNS-permeability	-2.826
Metabolism	CYP2D6-substrate	No
Metabolism	CYP3A4-substrate	No
Metabolism	CYP1A2-inhibitior	Yes
Metabolism	CYP2C19-inhibitior	No
Metabolism	CYP2C9-inhibitior	No
Metabolism	CYP2D6-inhibitior	No
Metabolism	CYP3A4-inhibitior	No
Excretion	Total-Clearance	0.612
Excretion	Renal-OCT2-substrate	No
Toxicity	AMES-toxicity	No
Toxicity	Max.-tolerated-dose-(human)	0.273
Toxicity	hERG-I-inhibitor	No
Toxicity	hERG-II-inhibitor	No
Toxicity	Oral-Rat-Acute-Toxicity-(LD50)	1.969
Toxicity	Oral-Rat-Chronic-Toxicity-(LOAEL)	1.467
Toxicity	Hepato-toxicity	Yes
Toxicity	Skin-Sensitisation	No
Toxicity	T.Pyriformis-toxicity	0.431
Toxicity	Minnow-toxicity	2.255

It has a good log P value of 1.20 which is essential for showing drug-like properties, along with 4 acceptors and 2 donors (Table 6).

Conclusion

The present study of the interaction of DAPH with BMLN reveals a positive interaction with BMLN. The fluorescence quenching study showed that DAPH can change the microenvironment of the Trp residues of BMLN as a consequence of their positive interaction. Stern-Volmer plot indicates that DAPH forms a complex with BMLN in the ground-state. The binding constant (or stability) of the BMLN-DAPH complexes are determined from the double logarithmic plot and it showed moderately stable complexation (binding constant of 10^5 order) occurring between DAPH and BMLN under the experimental conditions. The change in Gibbs free energy is negative which indicates that the binding of DAPH with BMLN is spontaneously under the experimental temperatures. The signs of ΔH and ΔS indicate that the DAPH mainly van Der Waals interaction and hydrogen bonding forces of attraction during complexation with BMLN. These are further supported by molecular docking studies, where the Gibbs free energy is nearly the same value as calculated from the fluorescence quenching study. ADMET studies indicate that DAPH can be considered a potential drug molecule. As it binds with BMLN, therefore BMLN can be considered as a carrier (vehicle) of the potential drug molecule DAPH or BMLN can be useful to enhance their drug-ability in this early stage of the drug delivery process.

Acknowledgement

This research was supported by the Science and Engineering Research Board (SERB), India. AM acknowledges SERB for research grant ref: EEQ/ 2019/000194. The authors are also thankful to the Presidency University, Kolkata for providing laboratory and NMR facilities. MD acknowledge Prabhat Kumar College, Contai, West Bengal for providing laboratory facilities.

Conflict of interest

All authors declare no conflict of interest.

References

1 Newman DJ, Cragg GM & Snader KM, The influence of natural products upon drug discovery. *Nat Prod Rep*, 17 (2000) 215.

2 Matatiken D, Hoareau L, Kante M, Mougal J, Rene P, Rosalie M, Spiro R & Vidot F, Conservation and management of medicinal plants: Experiences from seychelles. *Asian Biotechnol Develop Rev*, 13 (2011) 61.

3 Cragg GM & Newman DJ, Natural products: A continuing source of novel drug leads. *Biochim Biophys Acta*, 1830 (2013) 3670.

4 Fabricant DS & Farnsworth NR, The value of plants used in traditional medicine for drug discovery. *Environ Health Perspect*, 109 (2001) 69.

5 Pakrashy S, Chakraborty S, Manna S, Nanda Goswami J, Bhattacharya B, Emmerling F, Mandal J, Misra S, Choudhury SM, Okla MK, Bose A, Maurya PK, Majhi A & Dolai M, Inhibition of Human Colorectal Cancer by a Natural Product 7-Acetylhorminone and Interactions with BSA/HSA: Multispectral Analysis and *In silico* and *In vitro* Studies. *ACS Appl Bio Mater*, 7 (2024) 3414.

6 Agrawal P, Nikhade P, Patel A, Mankar N & Sedani S, Bromelain: a potent phytomedicine. *Cureus*, 14 (2022) 1.

7 Ghensi P, Cucchi A, Bonaccorso A, Ferroni L, Gardin C, Mortellaro C & Zavan B, *In vitro* effect of bromelain on the regenerative properties of mesenchymal stem cells. *J Craniofac Surg*, 30 (2019) 1064.

8 Lam AR, Bazzi K, Valle SJ & Morris DL, Novel use of bromelain and acetylcysteine (BromAc®) for pleural involvement in pseudomyxoma peritonei, *Case Rep Oncol*, 14 (2021) 628.

9 Akhter J, Quéromès G, Pillai K, Kepenekian V, Badar S, Mekkawy AH, Frobert E, Valle SJ & Morris DL, The combination of bromelain and acetylcysteine (Bromac) synergistically inactivates sars-cov-2. *Viruses*, 13 (2021) 425.

10 Sengupta P, Sardar PS, Roy P, Dasgupta S & Bose A. Investigation on the interaction of Rutin with serum albumins: Insights from spectroscopic and molecular docking techniques. *J Photochem Photobiol B Biol*, 183 (2018) 101.

11 Lakowicz JR, Principles of fluorescence spectroscopy. *Springer*, 2006.

12 Valeur B,Molecular fluorescence: principles and applications. *John Wiley & Sons*, 2013.

13 Li X, Yang Z & Peng Y, The interaction of silver nanoparticles with papain and bromelain. *New J Chem*, 42(7) (2018) 4940.

14 Li X, Yang Z & Bai Y, Fluorescence spectroscopic analysis of the interaction of papain and bromelain with l-ascorbic acid, α-tocopherol, β-carotene and astaxanthin. *Int J Biol Macromol*, 107 (2018) 144.

15 Pakrashy S, Mondal PK, Paul S, Misra S, Mandal J, Dolai M & Majhi A, a comparison of binding interaction of angelicin and psoralen o bromelain a cysteine protease: Steady-statefluorescence, circular dichorism and molecular docking study. *Spectrochem Acta A,* 336 (2025) 125964.

16 Misra S, Paul S, Pakrashy S, Ghosh S, Naskar S, Maurya PK, Sardar PS, Venkateswaralu K, Bose A & Majhi A, De-Novo drug design of novel 1,2,3–triazole-naphthamide as an inhibitor of SARS-Cov-2 main protease: Synthesis, bioinformatics and biophysical studies. *Indian J Chem*, 62 (2023) 1001.

17 Ross PD & Subramanian S, Thermodynamics of protein association reactions: forces contributing to stability. *Biochemistry*, 20 (1981) 3096.

18 Regitz M, Hocker J & Liedhegener A, t-Butyl Diazoacetate. *Org Synth*, 48 (1968) 36.

19 Cui SL, Lin XF & Wang YG, Novel and efficient synthesis of iminocoumarins via copper-catalyzed multicomponent reaction. *Org Lett*, 8 (2006) 4517.

20 Chen Z, Jin S, Jiang W, Zhu F, Chen Y & Zhao Y, Multicomponent Synthesis of Iminocoumarins via Rhodium-Catalyzed C—H Bond Activation. *J Org Chem*, 85 (2020) 11006.

21 Xu L, Zhou T, Liao M, Hu R & Tang BZ, Multicomponent polymerizations of alkynes, sulfonyl azides, and 2-hydroxybenzonitrile/2-aminobenzonitrile toward multifunctional iminocoumarin/quinoline-containing poly (N-sulfonylimine) s. *ACS Macro Lett*, 8 (2019) 101.

22 Han T, Xie J, Chen F, Sze PW, Su X, Wang D & Tang BZ, Synthesis of Hybridized Nontraditional Intrinsic Luminescent Polymers with Ring-Openable Fused Heterocycles by Facile Multicomponent Polymerizations. *Macromolecules*, 56 (2023) 10016.

23 Zhao Y, Zhou Z, Liu L, Chen M, Yang W, Chen Q, Gardiner MG & Banwell MG, The copper-catalyzed reaction of 2-(1-hydroxyprop-2-yn-1-yl) phenols with sulfonyl azides leading to C3-unsubstituted N-sulfonyl-2-iminocoumarins. *J Org Chem*, 86(13) (2021) 9155.

24 Palanichamy K, Suravarapu SR & Kaliappan KP, An efficient copper-catalyzed three-component synthesis of 3-C-linked glycosyl iminocoumarins. *Synthesis*, 44 (2012) 1841.

25 Mandal PK, Copper-catalyzed one-pot synthesis of glycosylated iminocoumarins and 3-triazolyl-2-iminocoumarins. *RSC Adv*, 4 (2014) 5803.

26 Allouche A, Software News and Updates Gabedit — A Graphical User Interface for Computational Chemistry Softwares. *J Comput Chem*, 32 (2012) 174.

27 Pettersen EF, Goddard TD, Huang CC, Couch GS, Greenblatt DM, Meng EC & Thomas EF, UCSF Chimera—a visualization system for exploratory research and analysis. *J Comput Chem,* 25 (2004) 1605.

28 Kumar MS, Pakrashy S, Manna S, Maity Chowdhury S, Das B, Ghosh A, Sheikh AH, Dolai M & Das AK, Fluoregenic selective detection of Zn^{2+} using a pyrazole-ortho-vanilin conjugate: Insights from DFT, moilecular docking, bioimaging and anticancer applications. *Anal Methods*, 17 (2025) 2125.

29 Pakrashy S, Mandal PK, Dey SK, Choudhury SM, Alasmary FA, Almalki AS, Islam AM & Dolai M, Design of a Structurally Novel Multipotent Drug Candidate by the Scaffold Architecture Technique for ACE-II, NSP15, and Mpro Protein Inhibition: Identification and Isolation of a Natural Product to Prevent the Severity of Future Variants of COVID-19 and a Colorectal Anticancer Drug. *ACS Omega*, 7 (2022) 33408.

30 Pakrashy S, Mandal PK, Nanda Goswami J, Dey SK, Choudhury MS, Bhattacharya B, Emmerling F ,Alasmary FA & Dolai M, Bioinformatics and Network Pharmacology of the First Crystal Structured Clerodin: Anticancer and Antioxidant Potential against Human Breast Carcinoma Cell. *ACS Omega*, 7 (2022) 48572.

31 Dolai M, Pakrashy S, Ghosh AK, Biswas S, Konar S, Alasmary FA, Almalki AS & Islam MA, Competent DNA binder pentagonal bipyramidal Fe (II) complex executed as a proficient catalyst for primary carbamates production from alcohols and urea. *J Mol Struct*, 1274 (2023) 134584.

32 Das B, Pakrashy S, Das GC, Das U, Alasmary FA, Wabaidur SM, Islam MA & Dolai M, Fashionable Co-operative Sensing of Bivalent Zn^{2+} and Cd^{2+} in Attendance of OAc- by Use of Simple Sensor: Exploration of Molecular Logic Gate and Docking Studies. *J Fluoresc*, 32 (2022) 1263.

33 Pakrashy S, Majhi A & Maurya PK, Embelin as an alternative reference standard for Delta-9-Tetrahydrocannibinol. *Indian J Chem*, 63(4) (2024) 390.

34 Wang J, Wang W, Kollman PA & Case DA, Antechamber, An Accessory Software Package For Molecular Mechanical Calculations. *J Am Chem Soc*, 222 (2001) 2001.

35 Guex N & Peitsch MC, SWISS-MODEL and the Swiss-PdbViewer: An environment for comparative protein modeling. *Electrophoresis*, 18 (1997) 2714.

36 Gasteiger J & Jochum C, An Algorithm for the Perception of Synthetically Important Rings. *J Chem Inf Comput Sci*, 19 (1979) 43.

37 Pires DEV, Blundell TL & Ascher DB. pkCSM: Predicting small-molecule pharmacokinetic and toxicity properties using graph-based signatures. *J Med Chem*, 58 (2015) 4066.